*photonics*

*Article*

# LBFA: A Load-Balanced and Fragmentation-Aware Resource Allocation Algorithm in Space-Division Multiplexing Elastic Optical Networks

**Shengyu Zhang, Kwan-Lawrence Yeung and Along Jin ***

Department of Electrical and Electronic Engineering, The University of Hong Kong, Hong Kong, China; zhangsy@eee.hku.hk (S.Z.); kyeung@eee.hku.hk (K.-L.Y.)
* Correspondence: ajin@eee.hku.hk

**Abstract:** We consider a space-division multiplexing elastic optical network (SDM-EON) that supports super-channels (SChs). A Sch comprises a set of contiguous frequency slots on multiple cores in a multi-core fiber. The problem of finding a lightpath using SChs involves routing, modulation, spectrum and core assignment (RMSCA). To minimize the request blocking probability (RBP), two critical issues must be addressed. First, routing and modulation assignment (RMA) should not cause hotspots, or overutilized links. Second, spectrum and core assignment (SCA) should aim at minimizing fragmentation, or small frequency slot blocks that can hardly be utilized by future requests. In this paper, a pre-computation method is first proposed for better load balancing in RMA. Then an efficient fragmentation-aware SCA is proposed based on a new fragmentation metric that measures both the spectral and spatial fragmentation. With the enhanced RMA and SCA, a joint load-balanced and fragmentation-aware algorithm called LBFA is designed to solve the RMSCA problem. As compared with the existing algorithms, simulation results show that our LBFA provides significant reduction in RBP.

**Keywords:** elastic optical networks; fragmentation; load balance; space-division multiplexing

**Citation:** Zhang, S.; Yeung, K.-L.; Jin, A. LBFA: A Load-Balanced and Fragmentation-Aware Resource Allocation Algorithm in Space-Division Multiplexing Elastic Optical Networks. *Photonics* **2021**, *8*, 456. https://doi.org/10.3390/photonics8100456

Received: 27 September 2021
Accepted: 17 October 2021
Published: 19 October 2021



## 1. Introduction

Due to the emergence of cloud-based services, network operators are seeking a better solution to implement advanced network infrastructures such as network function virtualization. The simplest approach is to directly build these network architectures on the top of the optical network [1,2]. However, considering the large variety of the requirements for interconnections between data centers [3,4], it is inefficient to utilize a conventional fixed-grid WDM optical network to support these advanced network infrastructures. Thus, space-division multiplexing elastic optical networks (SDM-EONs) [5] were proposed as a promising solution for future optical networks. SDM-EONs utilize both space division multiplexing (SDM) [6] and elastic optical network (EON) [7] technologies. EONs solve the mismatch of granularities between the client and physical wavelength layers. Compared to a conventional fixed-grid wavelength division multiplexing network, where the available optical spectrum of a single-mode fiber is divided into fixed 50 GHz frequency slots (FSs), EONs apply much finer granularity, e.g., 12.5 GHz per FS [8]. If a connection request has a larger bandwidth requirement, multiple FSs can be allocated. This on-demand allocation capability greatly enhances the efficiency of optical spectrum allocation. SDM technologies increase the network capacity by exploiting the spatial diversity [9–12] to send data in parallel.

SDM-EONs can be achieved by using (i) multiple modes in a multimode fiber, (ii) multiple cores in a multicore fiber (MCF), or (iii) both modes and cores in a few-mode multicore fiber (FM-MCF). Due to fine spatial switching granularity and similar attenuation properties as those of the single-core fiber [6], the weakly coupled MCF was widely adopted in the studies of SDM-EONs [5,13,14]. Benefitting from joint processing, amplifying, and switching, superchannels (SChs) that comprise a set of contiguous FSs on multiple cores can be realized in MCF [9,15]. The intercore crosstalk, which is generally inversely proportional to the core pitch, can be compensated using multi-input–multioutput (MIMO) at the cost of increased receiver complexity and energy consumption [16]. The problem of allocating resources to the SCh involves *routing, modulation, spectrum,* and *core assignment* (RMSCA) [5,13,14], and many algorithms have been designed to solve this problem. Typically, these solutions consist of four parts: (i) finding a route between source and destination nodes, (ii) selecting a modulation format according to the distance of the route, (iii) choosing the core(s) along the route to carry the optical channel, and (iv) allocating enough adjacent FSs to meet the bandwidth requirement. In a dynamic scenario where connection requests arrive in real time, an efficient RMSCA algorithm is of paramount importance.

The simplest approach to assign the route and the modulation format to an SCh is to use the predetermined shortest paths [5,16]. However, the shortest-path algorithm finds all routes with the lowest bandwidth consumption while ignoring the distribution of traffic load. Common links, utilized by different shortest paths, would be used more frequently. Thus, these links would bear a much higher load than that of other links and turn into bottleneck links. These bottleneck links in turn cause request blocking in dynamic scenarios. Network resources can be allocated more effectively if the routing schemes consider the load situation and avoid links with high loads. To find the load-balanced path in real time, a rule of thumb is to find the least loaded path from the source to destination. With the recent advances in multiprotocol label switching (MPLS) and software-defined networking (SDN) [17,18], real-time network status, including traffic load, is available at the central controller. So, when a connection request arrives, the controller can find the least loaded path to carry the request, such that the request blocking probability (RBP) is minimized. This strategy is called load-balanced routing and modulation assignment (LB-RMA).

In EONs, improper spectral assignment may cause small FS blocks that are hard to be utilized for future incoming requests, namely, fragmentation [19]. Fragmentation is a key limitation in achieving better network performance in EONs. In SDM-EONs, an on-demand spectrum and core allocation method was designed in [20] to reduce spectral fragmentation at the cost of the flexibility in spectral allocation. In [21], fragmentation could be reduced by allocating SChs just at the border of already occupied FSs. However, both methods were designed for allocating spectral SChs that are realized with only one core on each fiber. SChs that comprise a set of contiguous FSs on multiple cores may both spectrally and spatially produce fragmentation (see Section 3.2). To deal with the fragmentation problem in spectrum and core assignment (SCA) for SChs, we first investigate a fragmentation metric to measure both spectral and spatial fragmentation in SDM-EONs. Then, on the basis of this metric, a fragmentation-aware SCA strategy is proposed by finding the assignment that incurs the lowest fragmentation.

By jointly considering the two above strategies, we propose a load-balanced and fragmentation-aware algorithm, LBFA, to effectively solve the RMSCA problem for a lightpath with SChs in SDM-EONs. LBFA is realized by finding the least loaded path to carry the request, and selecting the best SCA to minimize spectral and spatial fragmentation. Simulation results show that, compared with the benchmark algorithm proposed in [5], our LBFA algorithm can achieve tremendous improvement in RBP and spectral efficiency in SDM-EONs.

The rest of this paper is organized as follows. In Section 2, related work is reviewed. In Section 3, network and request models are presented. On that basis, the LBFA heuristic algorithm was designed and is outlined in Section 4, and performance is compared in Section 5 by simulations. Lastly, we conclude the paper in Section 6.

## 2. Related Works and Contributions

### 2.1. Related Works

The routing and spectrum allocation (RSA) problem in EONs can be divided into two types, static/offline and dynamic/online. In the static RSA problem [22,23], the traffic matrix that indicates the traffic demands among all node pairs is given. With load balancing in mind, the goal is to place all demands in the network to minimize the highest FS index allocated to all links in the network. Although static RSA problems can be optimally solved by integer linear programming (ILP) [22], heuristic algorithms [23] can find a solution much faster, especially for large networks.

The dynamic RSA problem [17,19,24–29] considers real-time connection requests, and the goal is to minimize the RBP. Aiming at minimizing spectral consumption on the route, the shortest path routing algorithm was proposed in [24]. In [17], two heuristic algorithms were proposed for finding paths from a set of predetermined K-shortest paths. By allowing for a connection's traffic to be split over multiple paths, a multipath provisioning algorithm was also designed [25].

In [17,24,25], candidate paths for provisioning a connection request were predetermined to minimize the amount of real-time computing. Common links, utilized by different shortest paths, would be used more frequently. Thus, these links would bear a much higher load than that of other links and turn into bottleneck links. Bottleneck links, in turn, cause request blocking in dynamic scenarios. Aiming at allocating the spectrum resource more efficiently, a load-balanced RSA scheme was proposed in [26].

The fragmentation issue is another limitation in the EON. The improper selection among different available spectral blocks would cause small FS blocks that are hard to be utilized for future incoming requests. These small FS blocks are called fragmentation. To alleviate the fragmentation problem in EONs, several metrics were proposed to measure fragmentation [19,27–29]. In [27], fragmentation was evaluated by a metric called fragmentation ratio, which is defined as the ratio of the maximal data rate, providable using the available FS blocks, and providable if the same number of free slots was contiguous. In [28], fragmentation was measured by the number of continuous FS blocks. In [29], fragmentation was predicted by the metric "cut", which is defined as the break of continuous FS blocks. A route-based metric was proposed in [19], which considers the likelihood that an end-to-end FS block is large enough to provision a new connection. On the basis of these metrics, corresponding heuristic algorithms were proposed to minimize the fragmentation in RSA.

In SDM-EONs based on few-mode fibers, the static RMSCA problem was studied in [30]. In [31], an ILP was formulated, and a faster crosstalk-aware heuristic was proposed. More recently, the dynamic version of the RMSCA problem was studied [32]. Considering the fragmentation problem, in [20], an on-demand spectrum and core allocation method was designed. This method reduces spectral fragmentation by allocating a uniform bandwidth connection for each core. In [21], several fragmentation metrics were evaluated in SDM-EONs to achieve lower RBP. All these studies focused on the connection [20,21,30–32] assuming that only one mode or core could be utilized by each connection request.

In [15], a resource allocation model for spectral and spatial SChs (i.e., SChs that comprise a set of contiguous slots) was first introduced. Under this model, the static RMSCA problem was studied in [33], where a path-based ILP was formulated, and a stepwise greedy algorithm was designed. In [16], a three-dimensional resource assignment algorithm was proposed for solving the dynamic RMSCA problem in SDM-EONs based on FM-MCFs. Aiming at minimizing the wasted FSs, a sorting algorithm for selecting proper FS allocation pattern (FSAP) was proposed in [5].

### 2.2. Our Contributions

The routing and modulation format assignment (RMA) in all these studies [5,15,16,33] was predetermined by a shortest-path algorithm (or K-shortest paths). It is easy for the shortest-path algorithm to overutilize some bottleneck links, and this contributes to higher blocking probability. Moreover, spectral and spatial SChs are more likely to cause fragmentation in SDM-EONs, even if it is the FSAP that was proposed in [5], which attempted to reduce the internal FS waste of connection request, and achieved the state-of-the-art performance in providing SChs in SDM-EONs in the dynamic scenario. Fragments besides the occupied FSs are ignored. Thus, in this paper, aiming at better network performance (i.e., lower RBP), we propose a joint load-balanced and fragmentation-aware RMSCA algorithm in SDM-EONs. The specific contributions of this research work are as follows:

(1) We first jointly consider the load-balance and fragmentation issues in providing SChs in SDM-EONs.
(2) We propose a load-balanced RMA algorithm to solve the load-balance issue in providing SChs in SDM-EONs.
(3) We propose a fragmentation-aware SCA algorithm to solve the fragmentation issue in providing SChs in SDM-EONs.
(4) We evaluate our proposed algorithms via numerical simulation. Simulation results show that our proposed algorithm achieves state-of-the-art performance in providing SChs in SDM-EONs in a dynamic scenario.

## 3. System Model

The SDM-EON model is investigated in this section. On the basis of the SDM-EON model, the frequency slot allocation pattern (FSAP) proposed in [5] was utilized to establish spectral and spatial SChs. All notations used in this study are listed in Table 1.

**Table 1.** Notations in this study.

| Notion | Meaning |
|---|---|
| $G$ | Topology of SDM-EON. |
| $N$ | Set of nodes in an SDM-EON. |
| $L$ | Set of links in an SDM-EON. |
| $R$ | Set of requests. |
| $r$ | One connection request. |
| $s$ | Source node of a connection request. |
| $d$ | Destination node of a connection request. |
| $b$ | Information bit rate requirement of a connection request. |
| $t$ | Holding time of one request. |
| $q$ | Bandwidth requirement of a connection request in terms of the number of FSs. |
| $A$ | Number of stuffed FSs for one FSAP. |
| $W$ | Wasted FSs for one FSAP. |
| $p$ | Path of a connection request. |
| $B$ | Guard band measured by FSs. |
| $C$ | Set of cores on one fiber link in an SDM-EON. |
| $c$ | $c$-th core in the MFC. |
| $F$ | Set of FSs in one core on one link in an SDM-EON. |
| $f$ | $f$-th FS in the MFC. |
| $x^{l}_{(c,f)}$ | FS utilization at $f$-th FS layer in $c$-th core on link $l$. |

**Table 1.** *Cont.*

| Notion | Meaning |
|---|---|
| $M$ | Number of cores required to establish a spatial SCh. |
| $I$ | Number of FSs required by a connection request in each core. |
| $S$ | Index of starting FS of a connection request. |
| $E$ | Index of ending FS of a connection request. |
| $\alpha$ | Date rate for corresponding modulation format. |
| $\sigma_l$ | Traffic load on link $l$, $l \in L$. |
| $\lambda$ | Arrival rate of requests. |
| $\mu$ | Average holding time of requests. |
| $T$ | Entire simulation time. |
| $\Phi_f$ | Set of feasible cores under the spectrum assignment. |
| $X^*$ | Path-based FS allocation map. |
| $x^*_{(c,f)}$ | FS utilization at $f$-th FS layer in $c$-th core on path-based FS allocation map. |
| $\Psi$ | Core assignment of a request. |
| $\delta$ | Spectral utilization ratio during the entire simulation. |

### *3.1. Network Model*

An SDM-EON based on MCFs is modelled by an undirected graph $G(N, L)$, where $N$ is the set of nodes, and $L$ is the set of MCF links. The FSs of each MCF link $l \in L$ are represented by a two-dimensional array $(C, F)$, where $C$ is the set of cores in an MCF, and $F$ is the set of FSs in a core. We assumed that all the MCF links in the entire network were identical, e.g., 7-core MCF. For each $(c, f)$ on link $l \in L$, where $c \in C$ and $f \in F$, we define a bit mask $x^l_{(c,f)}$. If $x^l_{(c,f)} = 1$, the $f$-th FS of the $c$-th core on link $l$ is occupied by a lightpath; otherwise, $x^l_{(c,f)} = 0$ or the corresponding FS is free.

Each node in the network is a reconfigurable optical add/drop multiplexer (ROADM). From [34,35], EONs that support independent switching (Ind-Sw) with lane change require expensive large-scale optical cross-connections in each ROADM. To cut down on hardware cost, we assumed that a lane change was banned, i.e., all FSs on core $c_x$ of an incoming MCF must be switched together to the $c_x$ of an outgoing MCF. For FS blocks used by different lightpaths in the same core, a spectral guard band is needed at the end of each allocated FS block (see Figure 1) to mitigate the spectral nonlinearity between different connection requests unless $E + B \geq |F|$, where $E$ is the ending/highest FS index of an FS block and $B$ is the guard band requirement in FSs.

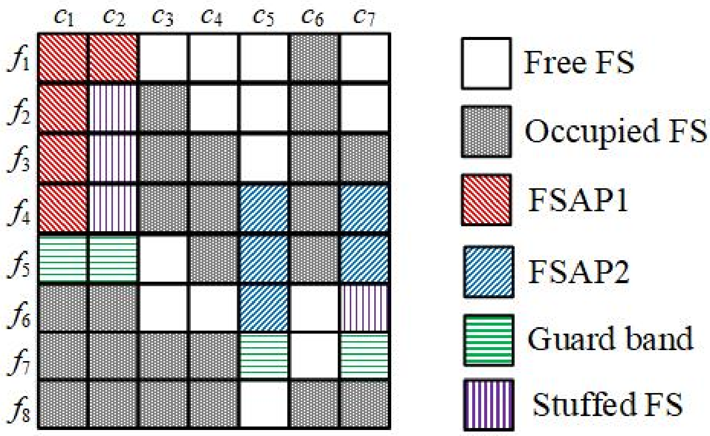


**Figure 1.** FS allocation map of 7-core MCF.

### 3.2. Request Model

Each request is denoted by $r(s, d, b)$, or a lightpath request from source $s$ to destination $d$ with an information bit rate requirement of $b$ bps. In this paper, we assumed that four modulation formats [36], namely, BPSK, QPSK, 8 QAM, and 16 QAM, could be used. The data rate ($\alpha$) and maximal transmission reach (TR) of each modulation format can be found in Table 2. When a modulation format ($m$) is chosen, bandwidth requirement$q$, expressed in terms of the number of FSs, is obtained as below:

$$q = \left\lceil \frac{b}{\alpha} \right\rceil. \tag{1}$$

When a connection request arrives, an algorithm (see Section 4) is used to find a lightpath to accept the request. When an ongoing connection ends, occupied FSs are released. In order to minimize disruption to ongoing connections, the repacking of ongoing lightpaths is not allowed.

**Table 2.** Date rate and transmission reach under different modulation formats [36].

| Modulation Format | Date Rate (Gbps) | Transmission Reach (km) |
|---|---|---|
| BPSK | 12.5 | 4000 |
| QPSK | 25 | 2000 |
| 8 QAM | 33.3 | 750 |
| 16 QAM | 50 | 400 |

### 3.3. Frequency Slot Allocation Pattern

To realize SChs that comprise a set of contiguous FSs on multiple cores, FSAP was proposed in [5] for minimizing the wasted FSs. Each FS allocation pattern (FSAP) is a rectangular FS block denoted by $(I, M)$, where $I$ is the number of contiguous FSs occupied in each core, and $M$ is the number of cores spanned. To minimize the scale of wavelength selective switch, one SCh should be allocated with the same contiguous FSs in different cores [5,16,20]. For a given bandwidth requirement of $q$, the request can be mapped to an FSAP only if $I \times M \geq q$. When $I \times M > q$, the excess and unused FSs should be padded to the FSAP to ensure that the same FS block is occupied in each core. The number of these padded FSs can be calculated as follows.

$$A = I \times M - q. \tag{2}$$

Consider the potential guard band in each core, wasted FSs $W$ in one FSAP can be calculated as:

$$W = B \times M + A. \quad (3)$$

Aiming at minimizing the wasted FSs, a sorting algorithm, ascending wasted FS (aW) policy, is proposed in [5]. The aW policy finds all feasible FSAPs to establish an SCh and sorts them by the ascending order of the potential wasted FSs of each FSAP.

For the example of $q = 5$, five FSAPs can be obtained, as shown in Figure 2a: $(I = 5, M = 1)$, $(I = 3, M = 2)$, $(I = 2, M = 3)$, $(I = 2, M = 4)$, $(I = 1, M = 5)$. $(I = 2, M = 4)$ is redundant because $(I = 2, M = 3)$ is a subset of $(I = 2, M = 4)$. Since $(I = 2, M = 3)$ is more efficient, it is always used instead of $(I = 2, M = 4)$. Then, wasted FSs are calculated by Equation (3), and the FSAPs are sorted by the ascending order of $W$. This means that an FSAP with a lower $W$ would be utilized to first establish the SCh. In this case, spectral efficiency is maximized. Figure 2b shows the sorting result for the same five FSAPs.

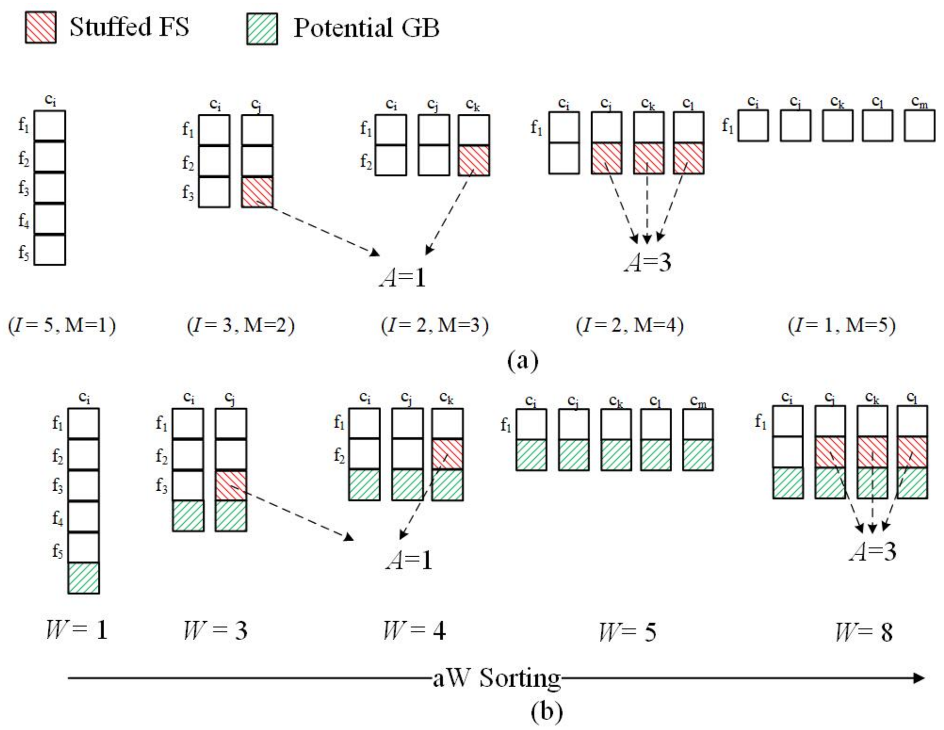


**Figure 2.** aW algorithm that was proposed in [5]: (**a**) all feasible FSAPs; (**b**) aW sorting strategy.

## 4. Our Approach

In this section, we first detail the load-balanced strategy in routing and modulation format assignment (LB-RMA), and the fragmentation-aware spectrum and core assignment (FA-SCA). Then, the load-balanced and fragmentation-aware algorithm (LBFA) is proposed by jointly considering the LB-RMA and FA-SCA strategies. Computation complexity is also analyzed.

### *4.1. Load-Balanced RMA*

Due to the mesh topologies of SDM-EONs, the predetermined shortest paths may more frequently use some links, and these links bear a much higher traffic load than that of other links. This eventually causes request blocking in dynamic scenarios. To find the load-balanced path in real time, a rule of thumb is to find the least-loaded path from the source to destination. With the recent advances on MPLS/SDN [17,18], real-time network status, including traffic load, is available at the central controller. So, when a connection request arrives, the controller can find the least-loaded path to carry the request, such that request blocking probability is minimized. This strategy is called LB-RMA.

Algorithm 1 shows the details of this LB-RMA. To find the least-loaded route, the traffic load on each link is first evaluated (lines 1–2). Using $x^l_{(c,f)}$ to represent spectral utilization on the link, the traffic load on each link ($\sigma_l$) can be calculated as:

$$\sigma_l = \sum_{c \in C} \sum_{f \in F} x^l_{(c,f)} \quad (4)$$

Using the traffic load on each link ($\sigma_l$) as the link cost (line 3), the least-loaded route can be found with the Dijkstra shortest-path algorithm (line 4). On the basis of path length and Table 2, the modulation format that gave the highest data rate was chosen and stored (line 5). The required FS was calculated by Equation (1) (line 6). Figure 3 shows an example of our proposed load-balanced RMA. Figure 3a shows a 3-core 6-node undirected topology. The slot block in Figure 3b represents the utilization of FSs in each fiber link, and $\sigma_l$ can be calculated according to the status of each link. Here is an incoming request $r(B, C, 200)$. In the conventional RMA, as shown in Figure 3c, the route with the minimal distance would be selected ($B \to C$). The FS requirement can be calculated through Equation (1), which is 4 slots. However, even taking advantage of modulation format, the incoming request is still blocked through the bottleneck link (Link $BC$). In Figure 3d, the traffic load on each link ($\sigma_l$) is calculated and assigned to each link. The least-loaded route is found by Dijkstra shortest path ($B \to A \to C$). The FS requirement can be calculated through Equation (1), which is 8 slots. We can easily allocate this request on Links $AB$ and $AC$.

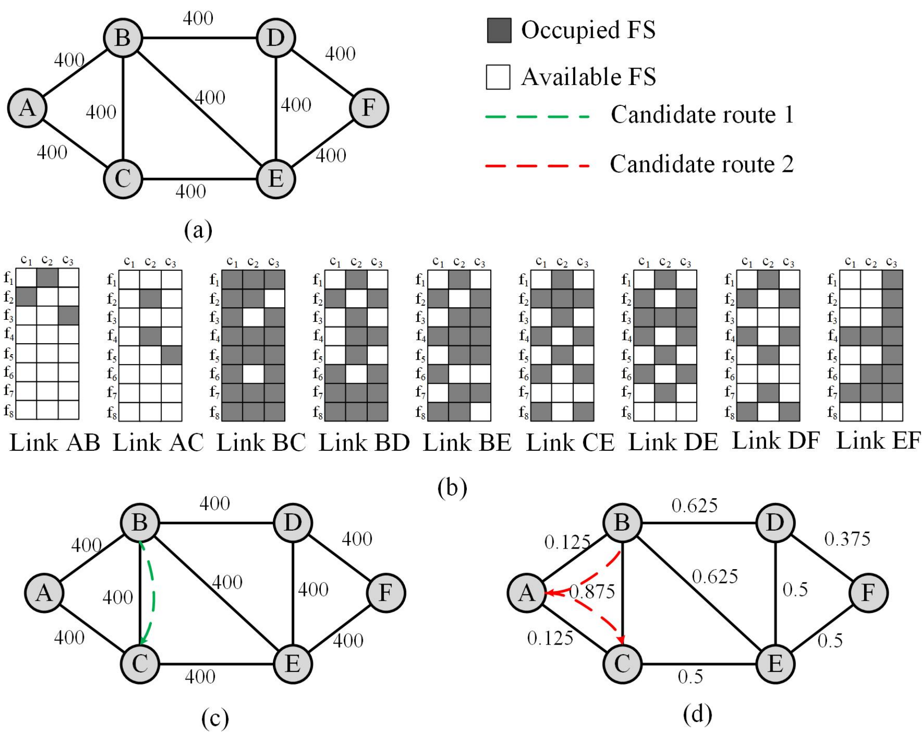


**Figure 3.** Illustration of LB-RMA: (**a**) 6-node topology; (**b**) link status in 6-node topology; (**c**) candidate route with shortest distance; (**d**) candidate route with least traffic load.

**Algorithm 1:** Load-balanced RMA

```
Require: Network topology G(N, L) and connection request r(s, d, b);
Ensure: Load-balanced path p, and bandwidth requirement q;
for all l ∈ L do
    Calculate traffic load σ_l by (7);
    Assign σ_l as link cost of l;
end for
Perform Dijkstra shortest path routing on G to find least-loaded path p;
Find feasible modulation format that gives highest data rate;
Calculate q by (1);
return p, q;
```

### 4.2. Fragmentation-Aware SCA

Fragmentation is one of the key limitations for network performance in EONs and SMD-EONs. SChs that comprise a set of contiguous FSs on multiple cores may both spectrally and spatially produce fragmentation. We assumed that the FSs possessed the same frequency index, but different core indices were neighbors. For example, $(c = 1, f = 10)$ and $(c = 2, f = 10)$ are neighbor FSs. Similarly, the same continuous FS blocks in different cores are neighbor FS blocks. SChs can only be established on neighbor FS blocks to save hardware cost [5,16]. If one FS block has few neighbors, there would be less possibility to provide future incoming traffic. In this case, the fragmentation problem should be considered both spectrally and spatially.

To minimize spectral and spatial fragmentation, the metric of cut proposed in [29] was adapted here to measure fragmentation. In [29], cut was defined as the candidate RSA solution that breaks the contiguousness of the FS blocks in EONs. In this study, we used the total number of cuts to predict the cost of the candidate spectral assignment solution. To establish an SCh with an FSAP $(I, M)$, for each index of starting FS, $S \in F$, all feasible cores that possessed enough continuous FS blocks to allocate the SCh were selected as $\Phi_f$. For each core in $\Phi_f$, we examined whether allocating an FS block with $I$ FSs would produce a cut. The total number of produced cuts is the cost of this spectral assignment solution. Here, the number of selected cores ($|\Phi_f|$) was no less than that of the required cores ($M$) in FSAP, $|\Phi_f| \geq M$. The additional cut in the extra cores was to limit the spatial fragmentation without additional cost. In this case, we considered both spectral and spatial fragmentation by one metric cut. The spectral assignment with the lowest cut was chosen, and cores with the lowest cut were selected. This is the fragmentation-aware SCA (FA-SCA).

Figure 4 shows an example of calculating cuts in spectral assignment for an FSAP $(I = 3, M = 2)$ in a 3-core SDM-EON. In Figure 4a, with candidate spectral assignment $S = 1$, no "cut" occurred, because the contiguousness of a spectral block in the three cores was not broken. In Figure 4b, with candidate spectral assignment $S = 5$, one "cut" occurred in the second core. In the first core, no cut occurred because the contiguousness of a spectral block in the three cores was not broken. In Figure 4c, with candidate spectral assignment S = 6, two "cuts" occurred in both of the first and second cores. In Figure 4d, with candidate spectral assignment S = 8, one "cut" occurred in the first core. This FSAP only requires 2 cores ($M = 2$) to establish the SCh, but all cuts on the feasible three cores were taken into account.

To simplify computing complexity, a path-based FS allocation map ($X^*$) [16] was obtained for routing assignment $p$ by superimposing the FS allocation maps of all links along the path (see Algorithm 2). On the basis of the FS allocation map ($X^*$), Algorithm 3 details the FA-SCA for a given FSAP. The total number of cuts for each spectral assignment was first calculated (lines 1–9). The feasible cores that possessed enough continuous FS blocks to allocate the SCh were selected into $\Phi_i$ (lines 5–6). Then, the spectral assignment with the lowest cut was selected to provide for the SCh (lines 10–11). Cores with the lowest cut in the spectral assignment were selected for core assignment (line 13–15).

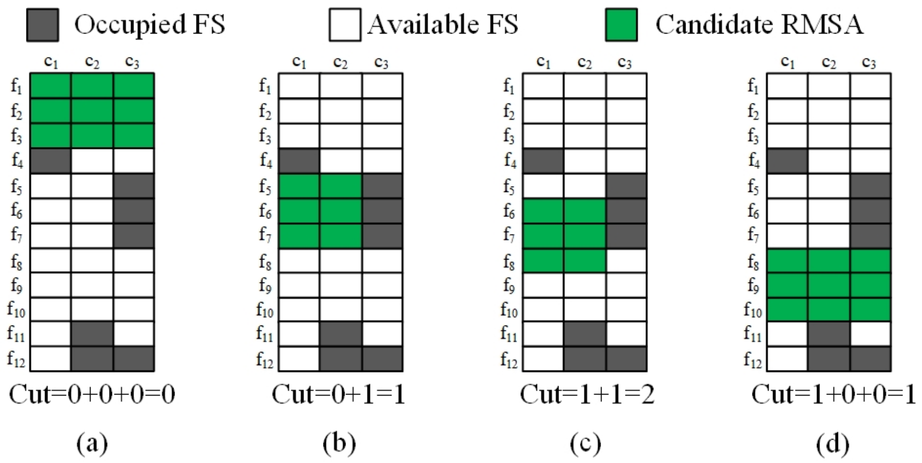


**Figure 4.** Examples of "cut" with different candidate spectral assignments: (**a**) S = 1, (**b**) S = 5, (**c**) S = 6, (**d**) S = 8.

---

**Algorithm 2:** Constructing path-based FS allocation map [16]

---

**Require:** Network topology $G(N, L)$ and route $p$;
**Ensure:** Path-based FS allocation map, $X^*$;
**for** all the $c \in C$ **do**
  **for** all the $f \in F$ **do**
    $x^*_{(c,f)} = 0$;
    **for** all the $l \in L$ **do**
      **if** $x^l_{(c,f)} = 1$ **then**
        $x^*_{(c,f)} = 1$;
      **end if**
    **end for**
  **end for**
**end for**
**return** $X^*$;

---

**Algorithm 3:** Fragmentation-aware SCA

---

**Require:** FS allocation map $X^*$ and FSAP, $(I, M)$;
**Ensure:** Spectrum assignment $S$ and core assignment $\Psi$;
$min = |C| + 1, i = 1$; /∗ initialize the spectrum and core assignment ∗/
**while** $i \neq |F| - I + 1$ **do**
  $cut\_count = 0$; /∗ initialize the cut counting ∗/
  **while** $j \neq |C|$ **do**
    **if** $\sum_{f=i}^{i+I-1} x^*_{j,f} = 0$ **then**
      Add $j$ into $\Phi_i$;
      **if** $x^*_{j,i-1} = 0$ & $x^*_{j,i+I} = 0$ **then**
        $cut\_count{+}{+}$;
      **end if**
    **end if**
    $j{+}{+}$;
  **end while**
  **if** $cut\_count < min$ & $|\Phi_i| \neq M$ **then**
    $min = cut\_count$ and $S = i$;
  **end if**
  $i{+}{+}$;
**end while**
**if** $min < |C| + I$ **then**
  Select $M$ cores with minimum "cut" from and record in $\Psi$;
**end if**
**return** $S$ and $\Psi$;

---

### 4.3. LBFA RMSCA

On the basis of load-balanced RMA and fragmentation-aware SCA, we propose a joint load-balanced and fragmentation-aware RMSCA (LBFA-RMSCA) solution. Algorithm 4 shows the details of our proposed joint algorithm. For an incoming request $r(s, d, b)$, a least-loaded route is first found by LB-RMA algorithm (line 2). All possible FSAPs would be found and sorted by the aW policy proposed in [5] (line 4). On the basis of FSAPs, the SCA with the lowest fragmentation is selected to provision this request (lines 5–11). If spectral resources in the network are not enough to be allocated, this connection request is blocked (line 13).

---

**Algorithm 4:** Joint LBFA-RMSCA Algorithm

---

**Require:** Network topology $G(N, L)$ and connection request $r(s, d, b)$;<br>
**Ensure:** Lightpath provision status;<br>
1: $Flag$ = False; /∗ initialize the lightpath provision flag ∗/<br>
2: Find route $p$, $q$ by Algorithm 1;<br>
3: Construct path-based FS allocation map $X^*$, by Algorithm 2;<br>
4: Find all feasible FSAPs of $q$ and sort them by the aW policy in [5];<br>
5: **for** all FSAP in ascending order of wasted FS (aW) **do**<br>
6:     Try to find spectral assignment $S$ and core assignment $\Psi$;<br>
7:     **if** found **then**<br>
8:         $Flag$ = True;<br>
9:         **break**;<br>
10:     **end if**<br>
11: **end for**<br>
12: **if** $Flag$ **then**<br>
13:     **return** Lightpath provision status ($p$, $q$, $S$, $\Psi$);<br>
14: **else**<br>
15:     **return** $\varnothing$ /∗This connection request is blocked∗/<br>
16: **end if**

---

### 4.4. Computation Complexity

When a connection request arrives, a lightpath can be established using Algorithm 4. Assume that the number of nodes is $|N|$, the number of links is $|L|$, the number of cores is $|C|$, the number of FSs is $|F|$, the maximal number of hops of the paths is $|p|$, and the maximal bandwidth requirement is $q$ in FSs.

For the route assignment, computation complexity for the calculation of $\sigma_l$ was $O(|L| \times |C| \times |F|)$, and computation complexity for the Dijkstra shortest path routing was $O(|N|^2)$. Total complexity of the LB-RMA was $O(\max\{|N|^2, |L| \times |C| \times |F|\})$.

For each path, the complexity of constructing the path-based FS allocation map was $O(|L| \times |C| \times |F|)$. The number of feasible FSAPs was $|C|$. The complexity of the FA-SCA was $O(|C| \times |F| \times q)$. Thus, the time complexity of our proposed LBFA was $O(\max\{|N|^2, |L| \times |C| \times |F|, |C|^2 \times |F| \times q\})$.

For comparison, the aW algorithm [5] has time complexity of $O(\max\{|N|^2, |L| \times |C| \times |F|, |C|^2 \times |F| \times q\})$, which is the same as that of our proposed LBFA-RMSCA algorithm.

## 5. Simulation Result

Without loss of generality, two network topologies, 12-node JP network in Figure 5a and 24-node USNET in Figure 5b, were simulated. In the USNET, shortest paths between some node pairs are longer than 4000 km, the maximal transfer reach of BPSK in Table 2. We assumed that optical repeaters were deployed, such that BPSK could still be used. In our simulations, both 7-core and 12-core fibers were considered. Each fiber was bidirectional, the total number of FSs supported in each core was $|F| = 320$, and the spectral guard band was set to $B = 1$ FS.

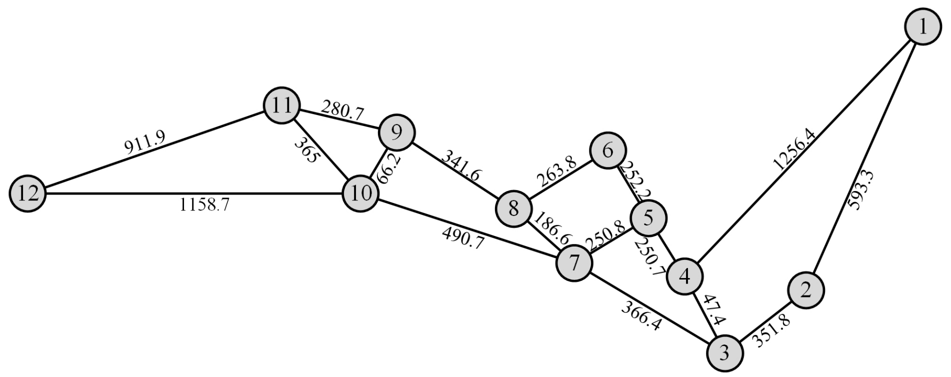


**(a)**

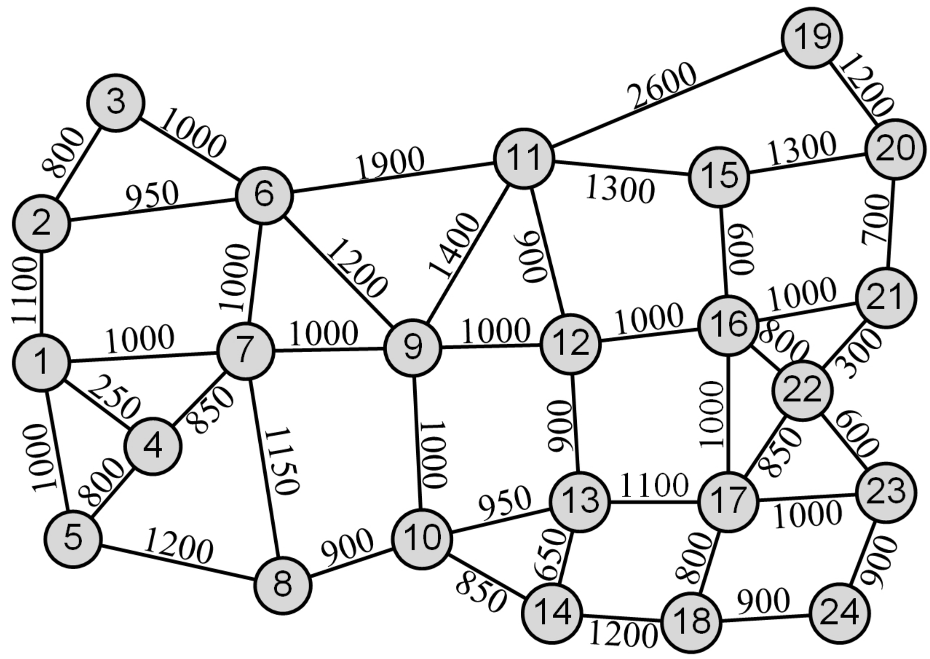


**(b)**

**Figure 5.** Two topologies: (**a**) 12-node JP network; (**b**) 24-node USNET.

We further assumed connection requests arrive following a Poisson process with an average of $\lambda$ requests per time unit and the connection holding time was exponentially distributed with an average value of $\mu$ time units. The bandwidth requirement of each request was uniformly distributed between 50 and 1000 Gbps or $b \in [50, 1000]$, and the source and destination of each request were randomly chosen among all nodes. Two performance metrics, RBP and spectral utilization ratio (SUR), are given in Figures 6 and 7. Each data point in the figures was obtained by averaging over $10^6$ connection requests.

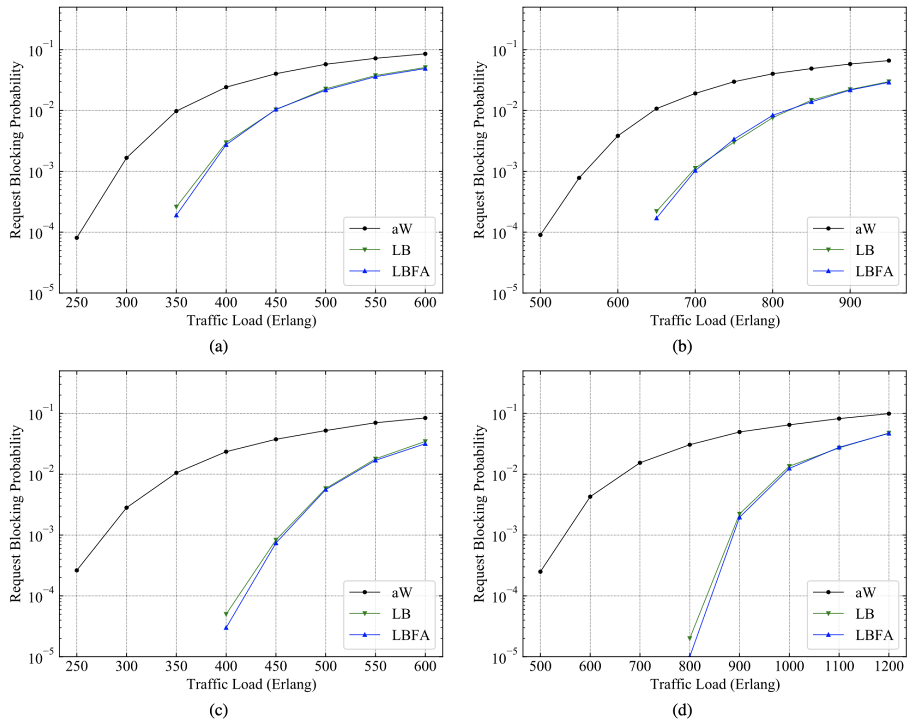


**Figure 6.** Request blocking probability versus traffic load: (**a**) 7-core JP network; (**b**) 12-core JP network; (**c**) 7-core USNET; (**d**) 12-core USNET.

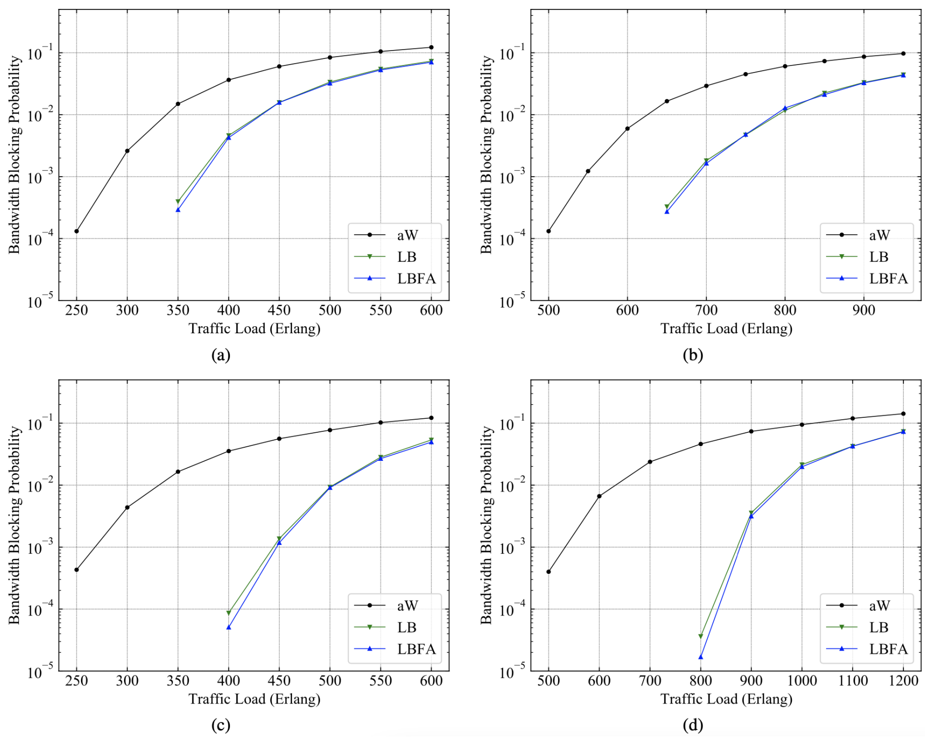


**Figure 7.** Bandwidth blocking probability versus traffic load: (**a**) 7-core JP network; (**b**) 12-core JP network; (**c**) 7-core USNET; (**d**) 12-core USNET.

For comparison, the aW policy proposed [5] was implemented as the benchmark algorithm. Two algorithms were adopted, LB (only considers the load-balanced RMA) and LBFA (jointly considers load-balanced and fragmentation-aware RMSCA).

Figure 6a shows RBP performance in the JP network with 7-core fiber link. When the LB-RMA strategy was used, LB outperformed aW. At low traffic load, the RBP of LB was more than an order of magnitude smaller than that of aW; at high traffic load, LB still achieved up to 2× lower RBP than aW. This shows that choosing the least-loaded route offers a clear advantage in RBP. Moreover, due to the additional effort on the fragmentation-aware SCA, LBFA had a lower RBP than LB under low traffic load (from 350 to 400), by up to 2×. As traffic load increased, however, the SCA is less flexible to avoid fragmentation. The difference between the RBP of LB and LBFA algorithms is negligible.

Figure 6c shows RBP performance in the 7-core, 24-node USNET. Compared with Figure 6a, the performance gap in RBP between our proposed algorithms and aW was larger. This is because the larger scale of the USNET makes traffic more concentrated on some bottleneck links. The load balance strategy can achieve better results. Lastly, Figure 6b,d show the performance in the 12-core JP network and USNET, respectively, and similar conclusions can be drawn. Without losing generality, we also show the simulation result of the bandwidth blocking probability (BBP) in Figure 7. As expected, the results of BBP were similar to those of RBP.

Our metric of interest was not only the RBP and BBP. We also evaluated the spectral utilization ratio ($\delta$) of our proposed joint LBFA–RMSCA algorithm. We assume that $R$ is the set of all the requests $r$ provisioned successfully in the simulation, $t$ is the hold time of each request $r$, $|p|$ is the hops of the route $p$ and $T$ is the entire simulation time. Then, $\delta$ could be obtained as follows.

$$\delta = \frac{\Sigma_{r \in R} I \times M \times t \times |p|}{|L| \times |C| \times |F| \times T} \tag{5}$$

Figure 8 shows the corresponding $\delta$ performance of that in Figure 6. LB and LBFA could achieve better spectral utilization than that of aW, especially at high traffic load (i.e., by up to 17%). This confirmed that the gain in RBP performance of our proposed algorithms (in Figure 6) was due to the efficient utilization of spectral resources.

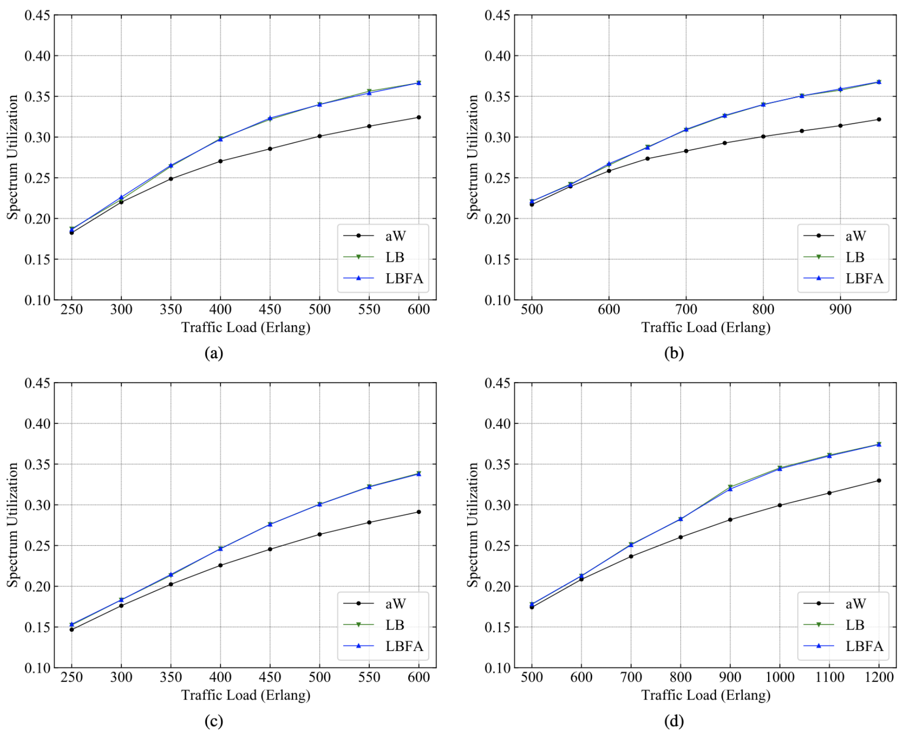


**Figure 8.** Spectral utilization ratio versus traffic load: (**a**) 7-core JP network; (**b**) 12-core JP network; (**c**) 7-core USNET; (**d**) 12-core USNET.

## 6. Conclusions

In this paper, we focused on achieving superior network performance, i.e., lower request blocking probability, in SDM-EONs. To this aim, a precomputation method based on the load balance strategy was first introduced as the RMA solution in SDM-EONs. We also investigated a fragmentation metric to measure both spectral and spatial fragmentation in SDM-EONs. A fragmentation-aware SCA was accordingly proposed. On the basis of these two strategies, we proposed a joint load-balanced and fragmentation-aware algorithm called LBFA to solve the RMSCA problem for a lightpath with SChs in dynamic scenarios. Simulation results show that, compared with the benchmark algorithm, our proposed load-balanced and fragmentation-aware RSCMA algorithm could achieve tremendous improvement in request blocking probability (e.g, up to 10× lower) and spectral efficiency (up to 17% higher) in SDM-EONs.

**Author Contributions:** Conceptualization, S.Z.; methodology, S.Z. and K.-L.Y.; validation, S.Z. and A.J.; formal analysis, A.J.; investigation, S.Z. and K.-L.Y.; data curation, A.J.; writing—original draft preparation, S.Z. and A.J.; writing—review and editing, K.-L.Y. and A.J.; visualization, A.J.; supervision, K.-L.Y. and A.J.; project administration, K.-L.Y. All authors have read and agreed to the published version of the manuscript.

**Funding:** This research received no external funding.

**Institutional Review Board Statement:** Not applicable.

**Informed Consent Statement:** Not applicable.

**Conflicts of Interest:** The authors declare no conflict of interest.

## References


1. Eramo, V.; Lavacca, F.G. Proposal and Investigation of a Reconfiguration Cost Aware Policy for Resource Allocation in Multi-Provider NFV Infrastructures Interconnected by Elastic Optical Networks. *J. Lightw. Technol.* **2019**, *37*, 4098–4114. [CrossRef]
2. Eramo, V.; Lavacca, F.G.; Catena, T.; Giorgio, F.D. Reconfiguration of Optical-NFV Network Architectures Based on Cloud Resource Allocation and QoS Degradation Cost-Aware Prediction Techniques. *IEEE Access* **2020**, *8*, 200834–200850. [CrossRef]
3. Eramo, V.; Lavacca, F.G. Computing and Bandwidth Resource Allocation in Multi-Provider NFV Environment. *IEEE Commun. Lett.* **2018**, *22*, 2060–2063. [CrossRef]
4. Eramo, V.; Lavacca, F.G. Optimizing the Cloud Resources, Bandwidth and Deployment Costs in Multi-Providers Network Function Virtualization Environment. *IEEE Access* **2019**, *7*, 46898–46916. [CrossRef]
5. Zhang, S.; Yeung, K.L. Dynamic service provisioning in space-division multiplexing elastic optical networks. *IEEE/OSA J. Opt. Commun. Netw.* **2020**, *12*, 335–343. [CrossRef]
6. Saridis, G.M.; Alexandropoulos, D.; Zervas, G.; Simeonidou, D. Survey and Evaluation of Space Division Multiplexing: From Technologies to Optical Networks. *IEEE Commun. Surv. Tutor.* **2015**, *17*, 2136–2156. [CrossRef]
7. Gerstel, O.; Jinno, M.; Lord, A.; Yoo, S.J.B. Elastic optical networking: A new dawn for the optical layer? *IEEE Commun. Mag.* **2012**, *50*, s12–s20. [CrossRef]
8. Jinno, M.; Takara, H.; Kozicki, B.; Tsukishima, Y.; Sone, Y.; Matsuoka, S. Spectrum-efficient and scalable elastic optical path network: architecture, benefits, and enabling technologies. *IEEE Commun. Mag.* **2009**, *47*, 66–73. [CrossRef]
9. Klonidis, D.; Cugini, F.; Gerstel, O.; Jinno, M.; Lopez, V.; Palkopoulou, E.; Sekiya, M.; Siracusa, D.; Thouénon, G.; Betoule, C. Spectrally and spatially flexible optical network planning and operations. *IEEE Commun. Mag.* **2015**, *53*, 69–78. [CrossRef]
10. Xia, T.J.; Fevrier, H.; Wang, T.; Morioka, T. Introduction of spectrally and spatially flexible optical networks. *IEEE Commun. Mag.* **2015**, *53*, 24–33. [CrossRef]
11. Mizuno, T.; Shibahara, K.; Ye, F.; Sasaki, Y.; Amma, Y.; Takenaga, K.; Jung, Y.; Pulverer, K.; Ono, H.; Abe, Y.; et al. Long-Haul Dense Space-Division Multiplexed Transmission Over Low-Crosstalk Heterogeneous 32-Core Transmission Line Using a Partial Recirculating Loop System. *J. Lightw. Technol.* **2017**, *35*, 488–498. [CrossRef]
12. Nakajima, K.; Sillard, P.; Richardson, D.; Li, M.; Essiambre, R.; Matsuo, S. Transmission media for an SDM-based optical communication system. *IEEE Commun. Mag.* **2015**, *53*, 44–51. [CrossRef]
13. Klinkowski, M.; Zalewski, G. Dynamic crosstalk-aware lightpath provisioning in spectrally-spatially flexible optical networks. *IEEE/OSA J. Opt. Commun. Netw.* **2019**, *11*, 213–225. [CrossRef]
14. Zhu, R.; Samuel, A.; Wang, P.; Li, S.; Li, L.; Lv, P.; Xu, M. Survival Multipath Energy-Aware Resource Allocation in SDM-EONs During Fluctuating Traffic. *J. Lightw. Technol.* **2021**, *39*, 1900–1912. [CrossRef]
15. Cvijetic, M.; Djordjevic, I.B.; Cvijetic, N. Dynamic multidimensional optical networking based on spatial and spectral processing. *Opt. Express* **2012**, *20*, 9144–9150. [CrossRef]

16. Arpanaei, F.; Ardalani, N.; Beyranvand, H.; Alavian, S.A. Three-Dimensional Resource Allocation in Space Division Multiplexing Elastic Optical Networks. *IEEE/OSA J. Opt. Commun. Netw.* **2018**, *10*, 959–974. [CrossRef]
17. Casellas, R.; Munoz, R.; Fabrega, J.M.; Moreolo, M.S.; Martinez, R.; Liu, L.; Tsuritani, T.; Morita, I. Design and Experimental Validation of a GMPLS/PCE Control Plane for Elastic CO-OFDM Optical Networks. *IEEE J. Sel. Areas Commun.* **2013**, *31*, 49–61. [CrossRef]
18. Gringeri, S.; Bitar, N.; Xia, T.J. Extending software defined network principles to include optical transport. *IEEE Commun. Mag.* **2013**, *51*, 32–40. [CrossRef]
19. Pederzolli, F.; Siracusa, D.; Zanardi, A.; Galimberti, G.; Fauci, D.L.; Martinelli, G. Path-based fragmentation metric and RSA algorithms for elastic optical networks. *IEEE/OSA J. Opt. Commun. Netw.* **2019**, *11*, 15–25. [CrossRef]
20. Fujii, S.; Hirota, Y.; Tode, H.; Murakami, K. On-demand spectrum and core allocation for reducing crosstalk in multicore fibers in elastic optical networks. *IEEE/OSA J. Opt. Commun. Netw.* **2014**, *6*, 1059–1071. [CrossRef]
21. Lechowicz, P.; Tornatore, M.; Wlodarczyk, A.; Walkowiak, K. Fragmentation metrics and fragmentation-aware algorithm for spectrally/spatially flexible optical networks. *IEEE/OSA J. Opt. Commun. Netw.* **2020**, *12*, 133–145. [CrossRef]
22. Klinkowski, M.; Walkowiak, K. Routing and Spectrum Assignment in Spectrum Sliced Elastic Optical Path Network. *IEEE Commun. Lett.* **2011**, *15*, 884–886. [CrossRef]
23. Christodoulopoulos, K.; Tomkos, I.; Varvarigos, E.A. Elastic Bandwidth Allocation in Flexible OFDM-Based Optical Networks. *J. Lightw. Technol.* **2011**, *29*, 1354–1366. [CrossRef]
24. Wang, Y.; Cao, X.; Pan, Y. A study of the routing and spectrum allocation in spectrum-sliced Elastic Optical Path networks. In Proceedings of the 2011 Proceedings IEEE INFOCOM, Shanghai, China, 10–15 April 2011; pp. 1503–1511. [CrossRef]
25. Lu, W.; Zhou, X.; Gong, L.; Zhang, M.; Zhu, Z. Dynamic Multi-Path Service Provisioning under Differential Delay Constraint in Elastic Optical Networks. *IEEE Commun. Lett.* **2013**, *17*, 158–161. [CrossRef]
26. Chen, X.; Li, J.; Zhu, P.; Tang, R.; Chen, Z.; He, Y. Fragmentation-aware routing and spectrum allocation scheme based on distribution of traffic bandwidth in elastic optical networks. *IEEE/OSA J. Opt. Commun. Netw.* **2015**, *7*, 1064–1074. [CrossRef]
27. Wang, R.; Mukherjee, B. Spectrum management in heterogeneous bandwidth networks. In Proceedings of the 2012 IEEE Global Communications Conference (GLOBECOM), Anaheim, CA, USA, 3–7 December 2012; pp. 2907–2911. [CrossRef]
28. Wright, P.; Parker, M.C.; Lord, A. Minimum- and maximum-entropy routing and spectrum assignment for flexgrid elastic optical networking [invited]. *IEEE/OSA J. Opt. Commun. Netw.* **2015**, *7*, A66–A72. [CrossRef]
29. Yin, Y.; Zhang, H.; Zhang, M.; Xia, M.; Zhu, Z.; Dahlfort, S.; Yoo, S.J.B. Spectral and spatial 2D fragmentation-aware routing and spectrum assignment algorithms in elastic optical networks [invited]. *IEEE/OSA J. Opt. Commun. Netw.* **2013**, *5*, A100–A106. [CrossRef]
30. Rottondi, C.; Boffi, P.; Martelli, P.; Tornatore, M. Routing, Modulation Format, Baud Rate and Spectrum Allocation in Optical Metro Rings With Flexible Grid and Few-Mode Transmission. *J. Lightw. Technol.* **2017**, *35*, 61–70. [CrossRef]
31. Yang, M.; Zhang, Y.; Wu, Q. Routing, spectrum, and core assignment in SDM-EONs with MCF: node-arc ILP/MILP methods and an efficient XT-aware heuristic algorithm. *IEEE/OSA J. Opt. Commun. Netw.* **2018**, *10*, 195–208. [CrossRef]
32. Tode, H.; Hirota, Y. Routing, Spectrum, and core and/or mode assignment on space-division multiplexing optical networks. *IEEE/OSA J. Opt. Commun. Netw.* **2017**, *9*, A99–A113. [CrossRef]
33. Yaghubi-Namaad, M.; Rahbar, A.G.; Alizadeh, B. Adaptive modulation and flexible resource allocation in space-division-multiplexed elastic optical networks. *IEEE/OSA J. Opt. Commun. Netw.* **2018**, *10*, 240–251. [CrossRef]
34. Marom, D.M.; Blau, M. Switching solutions for WDM-SDM optical networks. *IEEE Commun. Mag.* **2015**, *53*, 60–68. [CrossRef]
35. Marom, D.M.; Colbourne, P.D.; D'errico, A.; Fontaine, N.K.; Ikuma, Y.; Proietti, R.; Zong, L.; Rivas-Moscoso, J.M.; Tomkos, I. Survey of photonic switching architectures and technologies in support of spatially and spectrally flexible optical networking. *IEEE/OSA J. Opt. Commun. Netw.* **2017**, *9*, 1–26. [CrossRef]
36. Pincemin, E.; Song, M.; Karaki, J.; Zia-Chahabi, O.; Guillossou, T.; Grot, D.; Thouenon, G.; Betoule, C.; Clavier, R.; Poudoulec, A.; et al. Multi-Band OFDM Transmission at 100 Gbps with Sub-Band Optical Switching. *J. Lightw. Technol.* **2014**, *32*, 2202–2219. [CrossRef]